

## Research Article

# Investigation to Improve the Pool Boiling Heat Transfer Characteristics Using Laser-Textured Copper-Grooved Surfaces

Dharmendra Mani,<sup>1</sup> Suresh Sivan ,<sup>1</sup> Hafiz Muhammad Ali,<sup>2</sup> and Udaya Kumar Ganesan<sup>3</sup>

<sup>1</sup>Nanotechnology Research Laboratory, Department of Mechanical Engineering, National Institute of Technology, Tiruchirappalli 620015, India

<sup>2</sup>Department of Mechanical Engineering, King Fahd University of Petroleum and Minerals, Dhahran, Saudi Arabia

<sup>3</sup>Two-Phase Flow Laboratory, Department of Mechanical Engineering, Kookmin University, Seoul, Republic of Korea

Correspondence should be addressed to Suresh Sivan; [ssuresh@nitt.edu](mailto:ssuresh@nitt.edu)

Received 18 November 2019; Accepted 27 December 2019; Published 4 February 2020

Guest Editor: Chuanchang Li

Copyright © 2020 Dharmendra Mani et al. This is an open access article distributed under the Creative Commons Attribution License, which permits unrestricted use, distribution, and reproduction in any medium, provided the original work is properly cited.

Improving the performance of pool boiling with critical heat flux of pool boiling and enhancing the coefficient of heat transfer through surface modification technique have gained a lot of attention. These surface modifications can be done at different scales using various techniques. However, along with the performance improvement, the durability and stability of the surface modification are very crucial. Laser machining is an attractive option in this aspect and is gaining a lot of attention. In the present experimentation research work, pool boiling attributed performance of copper-grooved surfaces obtained through picosecond laser machining method is investigated. The performance of the modified surfaces was compared with the plain surface serving as reference. In this, three square grooved patterns with the same pitch (100  $\mu\text{m}$ ) and width (100  $\mu\text{m}$ ) but different depths (30, 70, and 100  $\mu\text{m}$ ) were investigated. Different depths were obtained by varying the scanning speed of the laser machine. In addition to the microchannel effect, the grain structuring during the laser machining process creates additional nucleation sites which has proven its effectiveness in improving the pool boiling performance. In all aspects, the pool boiling performance of the grooved laser-textured surface has showed increased surface characterisation as compared with the surface of copper.

## 1. Introduction

Pool boiling is a complex methodology associated with heat transfer in which the boiling surface is immersed and exposed to the pool of saturated liquid and the transfer of heat occurs on the heating element surface. It is also possible to enhance the heat transfer by surface modification [1]. The latent heat of vaporisation is the reason for the observation of high heat transfer coefficient that occurred in the boiling process. Nucleate boiling is a highly efficient process for removal of large quantities of heat from heated surface with minimal variation in surface temperature [2]. Notable applications of this process are two-phase heat exchangers and evaporators, boilers and steam generators, electronics cooling, nuclear fuel reactors, etc. [3]. The most important pool boiling heat transfer process techniques include heat transfer coefficient (HTC), superheat boiling incipience temperature, and the critical heat flux (CHF).

Efforts are made in process to lower various parameters which include increasing the CHF, boiling incipience superheat, and HTC [4].

In the past decades, researchers have focused much attention on the development of surface modification techniques. It is considered as the boiling phenomenon profoundly depends upon the surface and its interaction with the fluid used. The effect could enhance the pool boiling parameters of both the HTC and the CHF [5]. Surface modification at different scales is gaining a lot of attention among researchers to enhance the heat transfer characteristics of pool boiling. These structures modify the surface morphology, surface roughness, and the wettability of the surfaces. Although these techniques produce improved performance, their durability and endurance are a serious issue and this necessitates the application of durable surface modification methods. Laser machining is an effective method to modify the boiling surface, and many works are reported in this aspect [6].

The micro/nanostructure of pool boiling surfaces and the wettability effect on the surfaces can be altered using laser texturing. Functionalized metallic surfaces can be generated using an ultrafast picosecond laser processing technique which modifies the pool boiling heat transfer process by the creation of self-controlled micro/nanostructures by machining [7]. In this study, we focus on investigating the effect of cross-linked grooves in heat transfer associated with pool boiling. Most importantly, the effect of the depth of grooves is investigated in this experimental work. Grooves with constant width and pitch and with different depths were fabricated on copper surface using picosecond laser texturing. Investigation of surfaces processed with laser machining is already carried out by several researchers in the past, and they found improved pool boiling performance. Piasecka [8] conducted a study on the enhancement of heat transfer by boiling of FC-72. A laser microdrilling technique is applied in this technique to create a microchannel on the Haynes-230 alloy-based metal foil for flowing of FC-72, which could enhance the boiling performances. The 355 nm wavelength of a Nd:YAG laser emitting light is used to cover and drill the matrix of grooves on the Haynes-230 alloy-based metal foil. Materials melted as a circle-shaped layer that is micro grooved with input diameter as  $10\ \mu\text{m}$  and depth 3-2 as  $\mu\text{m}$  are uniformly arranged on both directions for every  $100\ \mu\text{m}$  which results in the boiling incipience that occurred for the heat fluxes inferior to the plain metal foil. This forms the augmentation of heat flux due to the boiling incipience which occurred earlier from the examined surfaces.

Sommers and Yerkes [9] investigated on the comparative studies in the enhancement of flow boiling performance via convective heat transfer using R-134a working fluid on aluminium surfaces through two distinct techniques: laser ablation and reactive ion etching. About 90-100% of pool boiling HTC is enhanced on Al metal surfaces by laser ablation. The laser-ablated surface pool boiling HTC is higher than the reactive ion-etched aluminium surface pool boiling HTC and also very higher than the bare metal surface. Kruse et al. [10] performed an experimental investigation on the functionalized multiscale micro/nanostructured metallic surfaces of pool boiling heat transfer. A femtosecond laser surface process (FLSP) technique is used for the fabrication of the mount-like multiscale micro/nanostructures, which are coated layer by layer by the self-arranged nanoparticles. The maximum CHF ( $142\ \text{W}/\text{cm}^2$ ) and the maximum HTC ( $67,400\ \text{W}/\text{m}^2\text{K}$ ) at  $29^\circ\text{C}$  are obtained for the processed samples. These obtained high CHF and high HTC are exaggerated by the increase of both nucleation associated with site density and surface areas. These are the highlighted major reasons for upgraded CHF and heat transfer.

Zupančič et al. [11] conducted a study on the effect of pool boiling on biphilic surfaces. The pool boiling effect is induced on the boiling surfaces by the formation of biphilic surfaces on stainless steel foil, which are fabricated using laser treatment. Initially, the pool boiling surfaces (stainless steel foil) are highly coated with hydrophobic coating in nature. Subsequently, the hydrophobic-coated boiling surfaces are surface modified by the laser treatment which gets

altered into superhydrophilic surfaces. A high CHF (350%) is achieved for the laser-treated biphilic surface than bare stainless steel foil. The nucleated bubble diameter is reduced, and further, the nucleation frequency is increased by the design of smaller hydrophobic spots. However, the boiling incipience and high HTC are promoted with larger hydrophobic regions at low heat fluxes. The homogeneous and inhomogeneous wettable surfaces are patterned on the surface of the boiling heat transfer by laser texturing, and the effect on homogeneous and inhomogeneous wettable surfaces is investigated. It is found that the enhancement of pool boiling behaviour is more effective and highly activated in inhomogeneous wettability [12].

Grabas [13] examined the heat transfer effect by pool boiling on laser-melted surface with  $\text{DDH}_2\text{O}$  as working fluid. This laser melting procedure has been found to modify the surface roughness of the boiling surface to a greater extent, and the result has been obtained as more than four-fold enhancement in the HTC and CHF. Recently, many other works were reported involving laser-treated surfaces and their effect on the pool boiling heat transfer technique. Hence, it is clearly stipulated that laser-treated surfaces are highly efficient in improving the pool boiling performance. Thus, this work provides a novel approach to study the effect of laser-treated surfaces to optimize the depth of the grooves using picosecond laser machining which changes the wettability of the working fluid to obtain superhydrophilic surface. This study conducts the pool boiling heat transfer studies on laser-textured surface with different depths of grooves and concluded the pool boiling heat transfer enhancement in contrast to bare copper surface.

## 2. Pool Boiling Experimental Setup

Experimentations were performed on copper surface with bare medium in association with laser-treated surfaces along the experimental setup which was modelled and fabricated to study the pool boiling characteristics involving with DI  $\text{H}_2\text{O}$  as working fluid. The experimental setup as shown in Figure 1 has the arrangements which include boiling chamber, heat input system, data acquisition system, and temperature and pressure modulator systems. The heat input arrangement consists of blocks of copper which are embedded with six cartridge heaters (WATLOW Firerod) on the bottom side of the copper block, so as to produce constant heat flux. Regulated DC power supply is used to operate the cartridge heaters to heat the copper block. To eliminate the heat losses in radial direction, the copper heater block was insulated with Teflon fittings which confirmed the conduction of heat flow for the temperature in one dimension at various heat fluxes. It can be ensured by its linearity which is obtained that  $R^2$  is 1 at various heat flux values. A stepped copper sample of 5 mm top radius was considered as test specimen. The bottom of the test specimen was perfectly aligned with high thermal conductive paste ( $k = 2.7\ \text{W}/\text{mK}$ ) on the top of the copper heater block of test specimen and heater block. Thereby, thermocouples (K-type) with a dimension of radius 0.5 mm and accuracy of  $\pm 0.5^\circ\text{C}$  were inserted to calculate the heat flux in axial direction of the

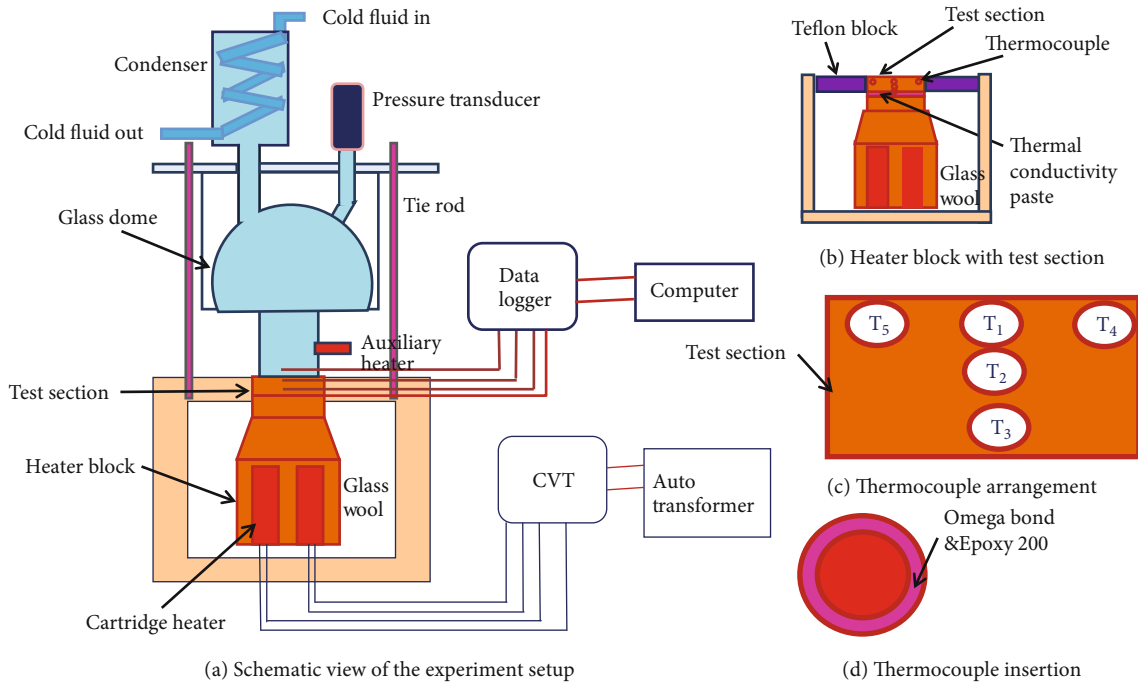


FIGURE 1: Pool boiling experimental setup.

copper test specimen. The copper specimen surface temperature can be observed by these readings from thermocouples; it is used to find out the heat flux, temperature gradient, and heat transfer coefficient as well.

Saturated condition of the water was attained by secondary heater (500 W) which is fixed inside the boiling chamber. The secondary heater is used to maintain the saturated critical point of boiling fluid by using a temperature controller which receives the temperature of boiling fluid through RTD. The chiller unit and condenser coil were used to maintain the boiling chamber in an atmospheric pressure condition by condensing the evaporating vapor, and this arrangement is used to maintain the boiling fluid of the chamber at standard level. During the experiments, pressure in the boiling chamber is continuously monitored by the pressure transmitter (WIKA, S-10). Thermocouple and pressure sensor readings were recorded by a data logger with the use of a computer. Condenser coil, pressure transmitter, and a RTD were strongly fixed in the chamber lid as well to avoid flow of vapor to the outside of the chamber.

### 3. Experimental Procedure

Initially, filled DI water in the boiling chamber was heated to remove noncondensable gases. After removal of gases, a chiller was employed to maintain the liquid level and the chamber pressure. As liquid reaches the saturation condition, the cartridge heaters were supplied with power. Bubble incipience event was captured by a high-speed camera. Once the boiling initiates, the temperature values were noted for all heat flux increment at steady state conditions. While taking reading, the auxiliary heater was switched off to avoid turbulence. A sudden temperature shoot in the surface was observed. Resemblance to the heat flux prior to the point is

considered as the critical heat flux. This procedure is repeated for all the modified surfaces, and the performance was compared. Thermal linear test was conducted in the heating chamber to confirm the one-dimensional heat conduction. Also, repeatability test was confirmed by carrying out the boiling test for three times for each individual surface.

### 4. Data Analysis

The copper heater block cylindrical side was tightly insulated with Teflon fitting and glass wool to ensure the conduction of heat in one dimension. The performance of pool boiling can be investigated with the help of heat flux, surface temperature, and heat transfer coefficient. As the experimental condition states, the heat conduction in one dimension results in determining the heat flux by calculating the gradient of temperature in axial direction of the testing specimen by Equation (1) [14]

$$q = -k \frac{dT}{dx}, \quad (1)$$

where  $k$  stipulates thermal conductivity of copper (390 W/mK), slope temperature ( $dT/dx$ ) can be retrieved from the approximation series (Taylor backward series) as in equation (2), and  $q$  is the critical heat flux to the projected area ( $W/cm^2$ ) of copper specimen.

$$\frac{dt}{dx} = \frac{3T_1 - 4T_2 + T_3}{2\Delta x}, \quad (2)$$

where temperatures of  $T_1$ ,  $T_2$ , and  $T_3$  can be calculated for the distance  $x$  between the thermocouples which are fixed axially along the copper test specimen (3 mm distance

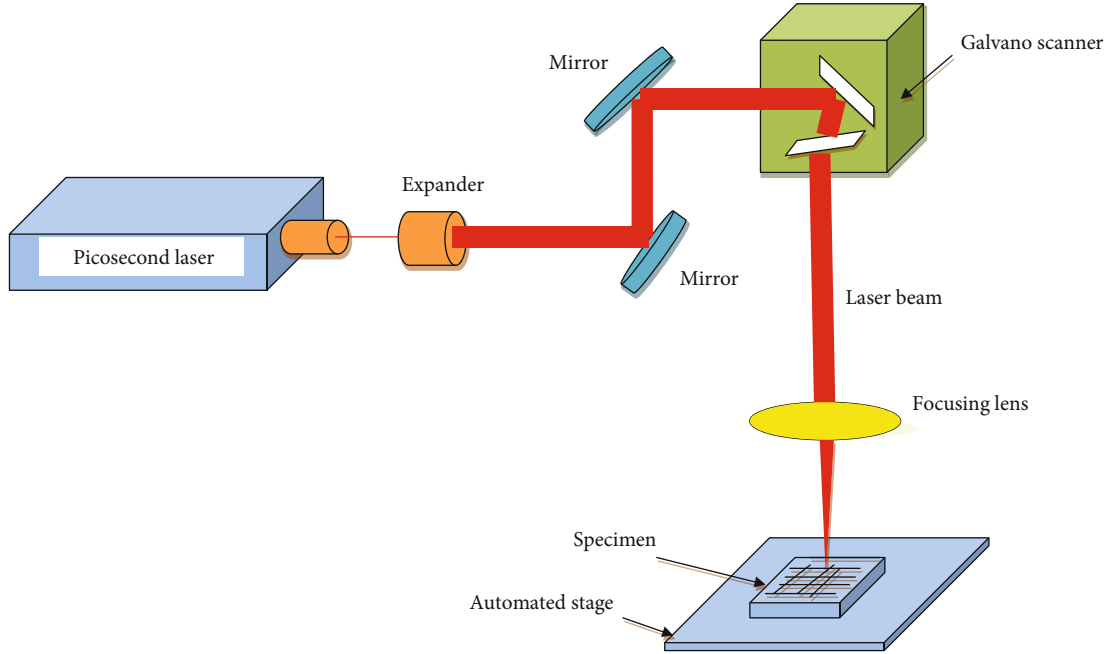


FIGURE 2: Schematic representation of the picosecond laser surface processing facility.

between  $T_1, T_2$  and  $T_2, T_3$ ). One-dimensional heat conduction equation can be rearranged to measure the surface temperature of the copper test specimen using Equation (3),

$$T_s = T_1 + q \frac{t}{K}. \quad (3)$$

$T_1$  is the measured temperature by the thermocouple which has been embedded at 3 mm distance from the top of the surface of the copper test specimen. Equation (4) is used to calculate the coefficient of heat transfer for convective boundary layer with respect to heat flux and temperature difference between surface and fluid [15].

$$h = \frac{q}{(T_s - T_f)}, \quad (4)$$

where  $T_s$  is the surface temperature and  $T_f$  is the temperature of the fluid at the saturated condition.

## 5. Fabrication of Modified Surface

A schematic representation of the picosecond laser facility is shown in Figure 2. To attain the grooved surfaces, picosecond-pulsed Nd:YAG laser with the wavelength 532 nm, pulse frequency 45 kHz, pulse width 650 ps, and beam diameter  $90 \mu\text{m}$  was employed in this study. The depth of the microgrooves was changed by varying the output power ( $0.7, 1.5, \text{ and } 2.9 \text{ J/cm}^2$ ) of the laser [1]. The output power of the picosecond laser was kept constant at 3 W and scanning speed at 30 mm/s. In this experiment, we have varied the number of pass as 1, 3, and 5 to obtain different depths. The specimens were placed on a programmable computer-controlled automated motion stage. During laser

TABLE 1: Dimensions of modified surfaces.

Name	Pitch ( $\mu\text{m}$ )	Width ( $\mu\text{m}$ )	Depth ( $\mu\text{m}$ )	No. of pass
LTs_1	100	100	30	1
LTs_2	100	100	70	3
LTs_3	100	100	100	5

structuring, the specimen was placed in a well-sealed chamber under ambient conditions. It should be noted that the samples are placed in atmospheric conditions before and after the laser irradiation. Scan separation line or pitch which is denoted by “a” resembles the distance between two adjacent laser lines. Similarly, width and depth of the laser lines are denoted as “w” and “d,” respectively. In this case, three modified surfaces with constant width and pitch and varying depths were used as shown in Table 1.

Figure 3 resembles the optical image of the laser-textured surfaces. We can clearly see the cross-linked grooved patterns. The wettability tests indicated that all the modified surfaces were hydrophilic in nature and the wettability has considerably increased as compared to the copper surface with plane textures.

Figure 4 shows scanning electron microscopy images of the laser-textured surface which were observed using SEM technique. Since LTs\_1 has a depth of 80 microns which is the least of the three samples, the melted copper flows without much obstruction which provides smooth surfaces (in other words, less protrusions or less relative roughness). However, the LTs\_2 sample has a depth of 100 microns which does not allow the flow easily. Hence, the resulting protrusions in these samples are more. In LTs\_3, the depth of the sample is further increased to 120 microns. Not only

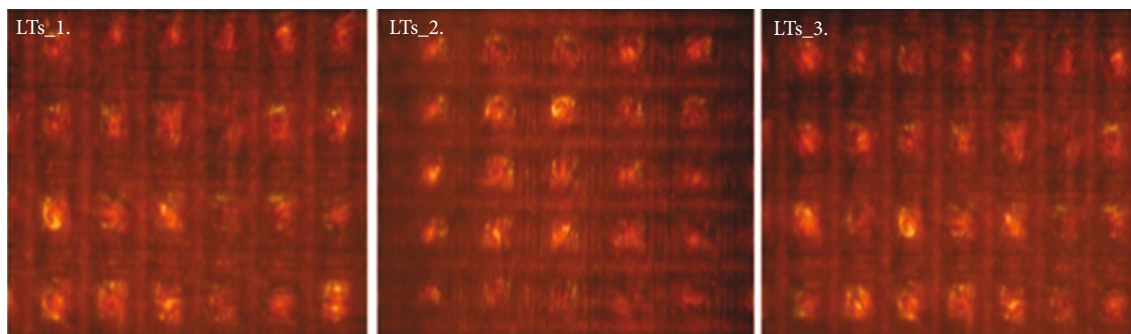


FIGURE 3: Optical images of laser-textured surfaces.

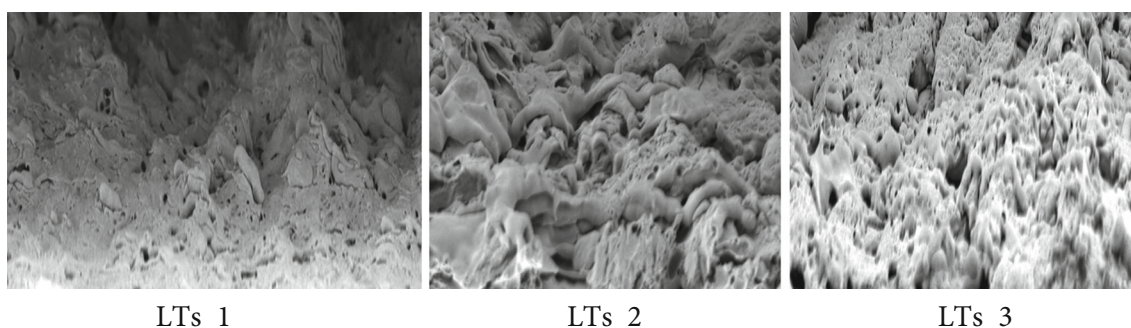


FIGURE 4: SEM images of laser-textured surface.

is the melted copper obstructed, but the dendrite formation also coagulated to form deeper protrusions (in other words, the relative roughness increases).

## 6. Results and Discussion

The basic objective is to enunciate the effect of pool boiling heat transfer characteristics on laser-textured grooved surfaces. These grooved surfaces have been fabricated using picosecond laser surface processing which formulates the surface roughness on both the micrometer and nanometer scales [16]. During the boiling process, cavities formed due to surface roughness which influences the bubble dynamics by removing the heat from the laser-textured surface. The depth of laser-textured surfaces was influenced by the density and size of the cavities. Thus, the role of the depth of laser-textured surfaces is interesting to examine the pool boiling heat transfer performance. Bare copper and three laser-textured surfaces with variable depth ( $\sim 30\ \mu\text{m}$ ,  $\sim 70\ \mu\text{m}$ , and  $\sim 100\ \mu\text{m}$ ) were used to conduct the experiments to observe the pool boiling performance. Experiments were conducted initially for very low heat flux, and further considerable increase of heat flux was incremented slowly until it reaches the critical heat flux in all sample surfaces.

Boiling performance of the laser-textured surfaces was compared by treating DI water as fluid with the baseline for the bare copper surface. Figures 5 and 6 clearly explain the performance of pool boiling for different laser-textured surfaces and bare copper surface. There is a drastic difference

between the heat transfer characteristics of processed and unprocessed surfaces which can be analysed through Figures 5 and 6. At every surface temperature, processed surface pool boiling performances were consistently improved than those of unprocessed surface. It is evidenced that the laser-textured surfaces have shown better boiling performance than bare copper surface as its curves moved towards leftward and upward.

Boiling incipience superheat initiates the bubble generation for the laser-textured surfaces at very low wall superheat values than bare copper surface as well. Figure 5 indicates that the boiling incipience which occurs in the bare copper surface was around  $10.9^\circ\text{C}$ ; equivalent heat flux of  $7.7\ \text{W}/\text{cm}^2$  but at  $7.0^\circ\text{C}$  boiling initiates for laser-textured surface LTs\_1 and further decreases with the increase in the depth of grid textured to  $6.3^\circ\text{C}$  and  $5.2^\circ\text{C}$  for corresponding laser-textured surfaces LTs\_2 and LTs\_3, respectively. The percentage of boiling incipience of the depth of the grid laser-textured surfaces is reduced with bare surface to 33.9%, 42.2%, and 52.2%, respectively.

Nucleation site density has the major role to reduce the percentage of boiling incipience superheat for laser-textured surfaces [17]. Due to laser texturing, melting of metal takes place which results into solidification as nanocrystals [18]. Also, the grooved area influenced the nucleation sites with increases in surface area. This increases the nucleation sites as a whole. Laser texturing on the copper surface increases the occurrence of a large number of cavities which produce the results as discussed above. These cavities increase the

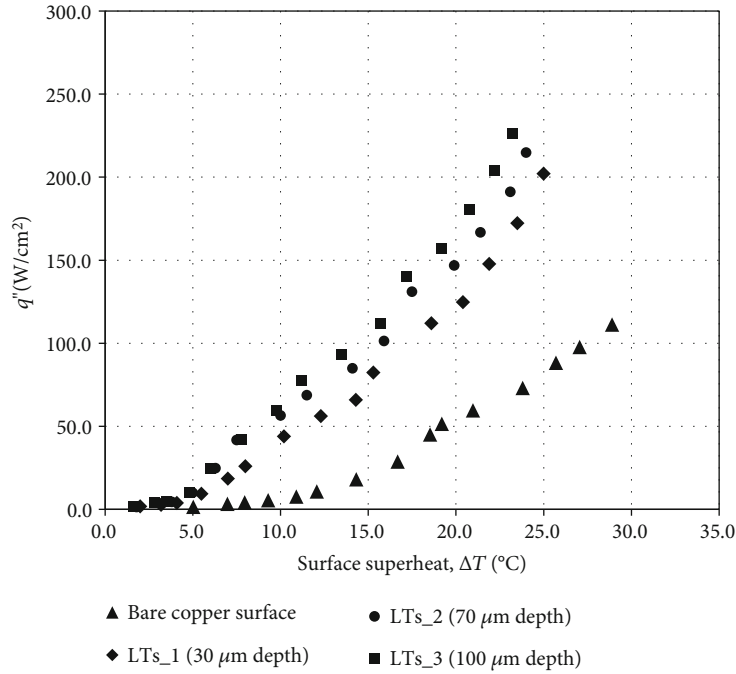


FIGURE 5: Heat flux variation with superheated surface for plain copper surface and laser-textured surfaces.

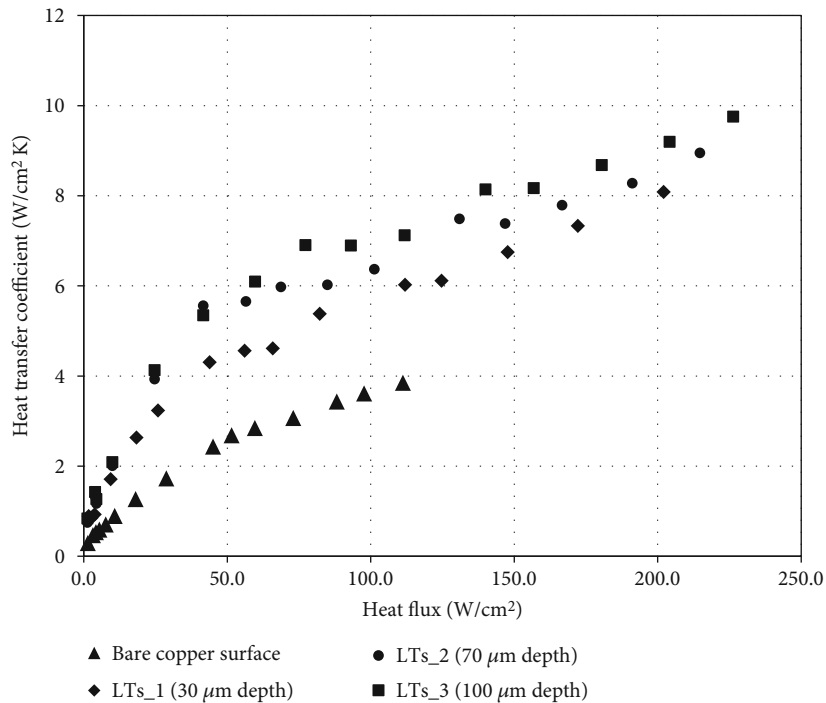


FIGURE 6: Heat transfer coefficient variation concerning with heat flux.

number of air entrapment sites which leads to the reduction of the percentage of the boiling incipience superheat. Nano- and microscale features on the processed surfaces increase the large number of micron-sized cavities which generate more nucleation sites that gets activated with lesser energy. The number of effective nucleation site can be increased while the depth of laser-textured surface increases with wide

range of cavity sizes. This formulates to create more active sites of nucleation easily under low surface superheat values. Safer limit to operate heat transfer enhancement in pool boiling technique was up to reach the CHF.

Figure 5 clearly indicates that the CHF values for the laser-textured surface are increased with reference to the bare copper surfaces. CHF for bare copper surface was  $111.3 \text{ W/cm}^2$  at

the superheated surface of 28.9°C, while the percentage increase of CHF for laser-textured surface is 81.5%, 92.9%, and 103.3% corresponding to the surfaces LTs\_1, LTs\_2, and LTs\_3, respectively. From Figure 5, the surface superheat temperature was reduced for different laser-textured surface. It is clearly observed that the bare copper surface significantly decreases in which the surface superheat was observed and this reduction is improved further with an increase in the depth of laser-textured surfaces. This obviously stated that the increasing depth of laser-textured surface has an optimistic effect on the improvement of CHF. Microstructure geometry can further explain the reason why laser-textured surface has more CHF values. From Figure 3, the area between the microstructures increases from the samples LTs\_1 to LTs\_3. Among the samples, LTs\_3 has more area by the formation network by densely packed deep valley structures, narrow channels, and micro cracks which formed between microstructures. During the machining, picosecond laser has settled more nanoparticles in the network channels of the microstructures on LTs\_3 due to its higher depth when compared to LTs\_2 and LTs\_1. It develops elevated capillary wicking effects to speedy top up the heated surface using cold fluid followed by the occurrence of local evaporation causing the delay of critical heat flux. Conversely, in other samples, channels are not formed properly due to increased microstructure size which results in deep pit formation between microstructures. Wicking potential of the surface is reduced due to the formation of deep pits and holes, and the presence of a nanoparticle layer covering the mound structure dominates the wicking effect. The highest CHF value of 226.3 W/cm<sup>2</sup> was observed in the LTs\_3 sample even if it had a larger peak valley height. But the wicking ability that is lacking due to the larger microstructure spacing of the LTs\_3 sample can be compensated by the dense microstructure of the surface area. Hence, the capillary wicking effect and surface wettability of the surfaces cause the enhancement of CHF for the laser-textured surface.

Laser-textured surfaces also enhance the value of heat transfer coefficient in comparison to the results shown for bare copper surface. From Figure 6, it clearly indicates that increasing the depth of laser texture on the copper surface increases the heat transfer coefficient and was found to be 3.85 W/cm<sup>2</sup>K. The percentage increase in the HTC for LTs\_1, LTs\_2, and LTs\_3 with bare copper surface is 109.9%, 132.4%, and 153.4%, respectively. The formation of microstructures during the picosecond laser machining on the copper surface acts like cooling fins to remove the heat from the surface. As the height of the microstructures increased, heat removal from the surface has also increased which has improved the cooling of the surface efficiently, and thus, HTC is increased. HTC's value is consistently higher for the LTs\_3 sample than the LTs\_1 and LTs\_2 samples. The overall enhancement of the HTC of the surface is promoted with an increase in the cavity density and capable nucleate boiling. The slope of the curves which increased over than the divergent point (120 W/cm<sup>2</sup>) is related with the peak valley height of the microstructure. It can be seen that the slope change in the curve increases with the increasing of the height of the microstructure. During high heat

fluxes, to activate the enhancement of heat transfer coefficients, laser-textured grooved surfaces are activated by the mixture of higher surface area ratio and prominent nature of tall microstructures as well as higher nucleation sites.

## 7. Conclusion

The experimental investigation for pool boiling heat transfer performance was studied by influencing the effect of depth in laser-textured grooved surfaces. Also, it results in the increases of CHF and HTC in the case of the laser-textured surfaces. It has been proved that the characteristics of CHF and heat transfer coefficients can be increased with the increase in depth of grooves of the laser-textured surface. The boiling incipience temperature is ultimately getting reduced by the cavities with micron size which act as nucleation sites for boiling.

## Data Availability

The data used to support the findings of this study are available from the corresponding author upon request.

## Conflicts of Interest

The authors declare that they have no conflicts of interest.

## Acknowledgments

The authors would like to acknowledge the ASME 2019 ICNMM 17th International Conference on Nanochannels, Microchannels, and Minichannels for accepting the topic in their prepresentation poster.

## References

- [1] D. Venkata Krishnan, G. Udaya Kumar, S. Suresh, M. Jubal, M. R. Thansekhar, and R. Ramesh, "Wetting transition in laser-fabricated hierarchical surface structures and its impact on condensation heat transfer characteristics," *International Journal of Heat and Mass Transfer*, vol. 140, pp. 886–896, 2019.
- [2] J. Voglar, M. Zupančič, A. Peperko, P. Birbarah, N. Miljkovic, and I. Golobič, "Analysis of heater-wall temperature distributions during the saturated pool boiling of water," *Experimental Thermal and Fluid Science*, vol. 102, pp. 205–214, 2019.
- [3] S. P. Rodrigues, C. F. A. Alves, A. Cavaleiro, and S. Carvalho, "Water and oil wettability of anodized 6016 aluminum alloy surface," *Applied Surface Science*, vol. 422, pp. 430–442, 2017.
- [4] A. Karthikeyan, S. Coulombe, and A. M. Kietzig, "Boiling heat transfer enhancement with stable nanofluids and laser textured copper surfaces," *International Journal of Heat and Mass Transfer*, vol. 126, pp. 287–296, 2018.
- [5] G. Liang and I. Mudawar, "Review of pool boiling enhancement by surface modification," *International Journal of Heat and Mass Transfer*, vol. 128, pp. 892–933, 2019.
- [6] L. Ventola, L. Scaltrito, S. Ferrero, G. Maccioni, E. Chiavazzo, and P. Asinari, "Micro-structured rough surfaces by laser etching for heat transfer enhancement on flush mounted heat sinks," *Journal of Physics: Conference Series*, vol. 525, no. 1, 2014.

- [7] H. S. Ahn, H. J. Jo, S. H. Kang, and M. H. Kim, "Effect of liquid spreading due to nano/microstructures on the critical heat flux during pool boiling," *Applied Physics Letters*, vol. 98, no. 7, article 071908, 2011.
- [8] M. Piasecka, "Flow boiling heat transfer in a minichannel with enhanced heating surface," *Heat Transfer Engineering*, vol. 35, no. 10, pp. 903–912, 2013.
- [9] A. D. Sommers and K. L. Yerkes, "Using micro-structural surface features to enhance the convective flow boiling heat transfer of R-134a on aluminum," *International Journal of Heat and Mass Transfer*, vol. 64, pp. 1053–1063, 2013.
- [10] C. M. Kruse, T. Anderson, C. Wilson et al., "Enhanced pool-boiling heat transfer and critical heat flux on femtosecond laser processed stainless steel surfaces," *International Journal of Heat and Mass Transfer*, vol. 82, pp. 109–116, 2015.
- [11] M. Zupančič, M. Steinbücher, P. Gregorčič, and I. Golobič, "Enhanced pool-boiling heat transfer on laser-made hydrophobic/superhydrophilic polydimethylsiloxane-silica patterned surfaces," *Applied Thermal Engineering*, vol. 91, pp. 288–297, 2015.
- [12] M. Zupančič, M. Može, P. Gregorčič, and I. Golobič, "Nano-second laser texturing of uniformly and non-uniformly wettable micro structured metal surfaces for enhanced boiling heat transfer," *Applied Surface Science*, vol. 399, pp. 480–490, 2017.
- [13] B. Grabas, "Vibration-assisted laser surface texturing of metals as a passive method for heat transfer enhancement," *Experimental Thermal and Fluid Science*, vol. 68, pp. 499–508, 2015.
- [14] G. Udaya Kumar, K. Soni, S. Suresh, K. Ghosh, M. R. Thansekhar, and P. Dinesh Babu, "Modified surfaces using seamless graphene/carbon nanotubes based nanostructures for enhancing pool boiling heat transfer," *Experimental Thermal and Fluid Science*, vol. 96, pp. 493–506, 2018.
- [15] M. Dharmendra, S. Suresh, C. S. Sujith Kumar, and Q. Yang, "Pool boiling heat transfer enhancement using vertically aligned carbon nanotube coatings on a copper substrate," *Applied Thermal Engineering*, vol. 99, pp. 61–71, 2016.
- [16] B. Wang, Y. Hua, Y. Ye, R. Chen, and Z. Li, "Transparent superhydrophobic solar glass prepared by fabricating groove-shaped arrays on the surface," *Applied Surface Science*, vol. 426, pp. 957–964, 2017.
- [17] C. H. Wang and V. K. Dhir, "On the gas entrapment and nucleation site density during pool boiling of saturated water," *Journal of Heat Transfer*, vol. 115, no. 3, pp. 670–679, 1993.
- [18] S. Vemuri and K. J. Kim, "Pool boiling of saturated FC-72 on nano-porous surface," *International Communications in Heat and Mass Transfer*, vol. 32, no. 1–2, pp. 27–31, 2005.